EFDA–JET–PR(07)20

M. Gatu Johnson, L. Giacomelli, A. Hjalmarsson, J. Källne, M. Weiszflog,
E. Andersson Sundén, S. Conroy, G. Ericsson, C. Hellesen, E. Ronchi,
H. Sjöstrand, G. Gorini, M. Tardocchi; A. Combo, N. Cruz, J. Sousa,
S. Popovichev and JET-EFDA contributors

The 2.5MeV Neutron Time-of-Flight Spectrometer TOFOR for Experiments at JET

The 2.5MeV Neutron Time-of-Flight Spectrometer TOFOR for Experiments at JET

M. Gatu Johnson[1,a], L. Giacomelli[1], A. Hjalmarsson[1], J. Källne[1], M. Weiszflog[1], E. Andersson Sundén[1], S. Conroy[1], G. Ericsson[1], C. Hellesen[1], E. Ronchi[1], H. Sjöstrand[1], G. Gorini[2], M. Tardocchi[2], A. Combo[3], N. Cruz[3], J. Sousa[3]; S. Popovichev[4] and JET-EFDA contributors*

JET-EFDA, Culham Science Centre, OX14 3DB, Abingdon, UK

[1]Uppsala University, Department of Neutron Research, 75120 Uppsala, Sweden (EURATOM-VR Association)
[2]Physics Department, Milano-Bicocca University, and Istituto di Fisica del Plasma del CNR, Milan, Italy (EURATOM-ENEA-CNR Association)
[3]Centro de Fusão Nuclear, Instituto Superior Téchnico, Av. Rovisco Pais 1, 1049-001 Lisboa, Portugal (Associação EURATOM/IST)
[4]Euratom/UKAEA Fusion Association, Culham Science Centre, Abingdon, Oxon, UK
** See annex of M.L. Watkins et al, "Overview of JET Results", (Proc. 21st IAEA Fusion Energy Conference, Chengdu, China (2006)).*

Preprint of Paper to be submitted for publication in
Nuclear Instruments and Methods in Physics Research Section A

ABSTRACT

A Time-Of-Flight (TOF) spectrometer for measurement of the 2.5MeV neutron emission from fusion plasmas has been developed and put into use at the JET tokamak. It has been Optimized for operation at high Rates (TOFOR) for the purpose of performing advanced Neutron Emission Spectroscopy (NES) diagnosis of deuterium plasmas with a focus on the fuel ion motional states for different auxiliary heating scenarios. This requires operation over a large dynamic range including high rates of >100kHz with a maximum value of 0.5MHz for the TOFOR design. This paper describes the design principles and their technical realization. The performance is illustrated with recent neutron time-of-flight spectra recorded for plasmas subjected to different heating scenarios. A data acquisition rate of 39kHz has been achieved at about a tenth of the expected neutron yield limit of JET, giving a projected maximum of 400kHz at peak JET plasma yield. This means that the count rate capability for NES diagnosis of D plasmas has been improved more than an order of magnitude. Another important performance factor is the spectrometer bandwidth where data have been acquired and analyzed successfully with a response function for neutrons over the energy range 1 to >5MeV. The implications of instrumental advancement represented by TOFOR are discussed.

1. INTRODUCTION

The neutron emission from fusion plasmas carries information about the condition of the neutron source, predominantly, the reactions d+t→α+n (E_n = 14MeV) and d+d→^{3}He+n (E_n = 2.5MeV) in DT and D plasmas, in terms of intensity and the motional state of the fuel ions, tritons and/or deuterons. The most detailed information is obtained from Neutron Emission Spectroscopy (NES) measurements, which require the use of instruments developed for the particular purpose of so-called plasma diagnosis. The main measurement figure of merit for advanced NES diagnosis is high count rate in combination with sufficient energy resolution. This is the necessary basis for achieving sufficient statistics during short times. Time resolved data collection is needed for observing variations in the neutron source conditions at the time scale they occur, spontaneously or induced. The present standard for advanced NES diagnostics is the achievements made at the JET tokamak for DT plasmas in 1997 with the MPR technique, i.e., measurements with a magnetic spectrometer of the proton recoils produced by neutron-proton (*np*) elastic scattering in a thin polythene foil placed in the collimated beam of neutrons from the plasma. The MPR operated at high count rates (C_n) only limited by the source intensity, i.e., the neutron yield rate Y_n, leading to a count rate of $C_n \approx$ 0.6 MHz when JET reached the peak fusion power of 16 MW or $Y_n \approx 6\times10^{18}$ n/s [1].

In order to perform advanced NES diagnosis of D plasmas, one needs a 2.5MeV spectrometer with a factor of 100 higher efficiency than a comparable 14MeV spectrometer to compensate for the difference in yield rate of dd compared to dt reactions for the same ion motional state. High efficiency is offered by the neutron Time-Of-Flight (TOF) technique. This is easier to implement for 2.5MeV dd fusion neutrons than for those of dt at 14MeV because the required energy resolution can be achieved with relatively short (≈1m) flight paths and because of the higher interaction cross

sections in the scintillators at lower neutron energies. The method is based, in this case, on two detectors, for instance, scintillators, of which one is placed in the beam (S1) and the other in a removed position (S2). The signals from S1 and S2 provide a "start" and a "stop" for time-of-flight measurements. The limit on the count rate is set by the tolerable admixture of random coincidences (accidentals). NES diagnosis of D plasmas has been performed with TOF spectrometers before [2,3] but with the operation limited to the few kHz range. Therefore, the success of advanced NES diagnosis demonstrated for DT plasmas [4] has motivated the present TOFOR project to create a TOF spectrometer Optimized for Rate to make this realizable for D plasmas. A special motivation for this effort is the fact that JET, as other tokamaks, operates routinely with D but is the only fusion reactor capable of T handling and operation.

A concept for a neutron TOFOR spectrometer has been presented in [5]. This showed that the TOF technique could, in principle, be developed to permit operation in the 100kHz range. The key element to focus on was identified to be the design of the S1 and S2 scintillators, specifically, to maximize within practical constraints the fraction of the neutrons that after interaction in S1 through *np* scattering were also detected in S2. This fraction was referred to as the neutron catching factor of the S2 detector, which was the parameter to optimize as it implied, for the targeted count rate, minimization of accidental admixture in the measured TOF spectrum [5 ,6, 7].

The TOFOR concept has been the object for development and design that has now been realized in an instrument. As with earlier TOF spectrometers, this has entailed the design of a system of two scintillator detectors, S1 and S2. The scintillator surfaces are configured to the geometry of a sphere so that the energy distribution of the incoming neutron flux can be determined from the measured time-of-flight spectrum independent of the neutron scattering angle. Here lies the key to optimizing the count rate capability limit. In order to approach this limit for the neutron fluxes that JET can produce, the efficiency was increased as much as possible, partially at the cost of worsened energy resolution. The energy resolution ($\Delta E_n / E_n$) should be on the scale of the thermal Doppler broadening for d+d neutrons from 4keV plasmas, i.e., $\Delta E/E \approx 7\%$ (FWHM using the neutron energy distribution function derived in [8]). Such an energy resolution is acceptable if the instrument can be calibrated to high accuracy and if the instrumental stability can be verified through suitable monitoring. This was, in part, provided by a special Control and Monitoring (C&M) system developed for this purpose. The Data AcQuisition (DAQ) was, for the first time in fusion neutron TOF spectrometry, based on a technique where the time trains of selected events in the S1 and S2 detectors were recorded for the duration of the plasma discharge (typically tens of seconds) and then used to construct TOF spectra for selected plasma time periods. This was implemented through time recording PC cards especially developed for this application, which contribute to raising the count rate capability limit of TOFOR to a projected level of 0.5MHz. Finally, the response of TOFOR to neutrons has been described with the help of detailed geometrical modeling and neutron transport calculations. Such calculations were used in the design of TOFOR as well as for the calibration represented by simulated TOF spectra for fluxes of neutrons of given energy in an arbitrary range around 2.5MeV; good sensitivity is predicted

for the energy range 1 to 5 MeV and lower sensitivity beyond.

This paper describes the design of the TOFOR spectrometer and the choices made to optimize the count rate. The roles of the C&M and DAQ systems are also described and their use for achieving the design targets. The performance of TOFOR is illustrated with recent results from measurements at JET. These include high-count rate operation, handling of accidental admixture in the data, exploitation of the TOFOR broadband capability and extraction of ion motion information from analysis of measured TOF spectra.

2. DESIGN PRINCIPLES

Since the fusion plasma is an extended and continuous source of neutrons, the use of the TOF method to determine the neutron energy requires the use of two detectors. With plastic scintillator detectors, the first (S1) is placed in a collimated beam of neutrons, a fraction of which is detected through the proton recoils produced in the scattering process $n + p \rightarrow p_R + n'$. The second detector (S2) is placed a known distance (L) away from S1 and records a fraction of the scattered neutrons, again through proton recoils (Figure 1).

The S1 and S2 detectors can be given different internal designs as well as configurations relative to each other. Regarding the latter, TOFOR was designed based on a geometry where the S1 and S2 detectors are placed on the constant TOF sphere (Figure 2) [5]. In this configuration, the flight time recorded for a passing scattered neutron ($t_{TOF} = t_2 - t_1$) is the same for incoming neutrons of a given energy independent of the scattering angle a. This comes from the angular dependence of the flight path given by $L = 2r\cos\alpha$. Within the assumptions of non-relativistic *np* scattering kinematics and $m_p \approx m_n$, the energy of the scattered neutron is given by $L = 2r\cos\alpha$ and related to the incident neutron energy through $En = E_{n'}/\cos^2\alpha$. Thus, E_n is determined from the measured t_{TOF} spectrum provided that the radius*r* is known, i.e., _____.

The coordinate system used to describe the TOFOR design is based on defining a system axis which goes through the point of entry for the incoming neutrons (I) and the origin (O) of the constant TOF sphere of radius *r* (Figure 2). The point of exit for a scattered neutron is defined by the polar angle ($\zeta = 2\alpha$) and the azimuthal angle *j*. The system is axis-symmetric for rotation in *j* but for the internal geometry of the S2 detector elements. The incoming neutron flux is defined by a cylindrical collimator whose axis coincides with the system axis. The TOFOR detectors have flat scintillators of finite volumes whose positions are given by the coordinates of the center of their area and half thickness point. This defines uniquely the coordinates of S1 as its surface is perpendicular to the axis. In the case of S2, the scintillator surfaces are perpendicular to the radius as its reference orientation. However, S2 can be tilted, which is used in the TOFOR design. The tilting (angle ÷ in Figure 2) partly compensates for the timing uncertainty introduced by the variation in light propagation time to the PM tube depending on interaction point.

In addition, special features to further enhance the achievable count rate were implemented for TOFOR:

- The S1 detector was segmented in five layers to allow for detection of more events without running into PM tube saturation.
- Specially developed PC cards were used to make dead-time free recording of all detected events possible.
- The C&M system was implemented as an integrated part of the instrument to allow for corrections for any drifts from the set working points.

Optimizing the TOFOR design included balancing the conflicting requirements on efficiency and energy resolution against each other, choosing the number of S1 detectors and determining the detectors sizes and the solid angle coverage of the S2 in a way so as to achieve maximum detection efficiency with keeping practical construction aspects in mind. The decisions were made based on results from neutron transport simulations [9] using the GEANT4 code [10]. The information obtained was used in the development of the TOFOR design including the size and number of detectors to use as well as their location relative to the constant TOF sphere. The 3D model of the 5 S1 and 32 S2 detectors of TOFOR is shown in Figure 3.

3. THE TOFOR INSTRUMENT

TOFOR was designed for installation at JET so as to view a collimated neutron flux coming up vertically from the plasma. It was built and tested as a fully assembled instrument at Uppsala University and transported to JET in parts. The design afforded disassembly and remounting within required alignment specifications. Survey and alignment performed during the construction phase were maintained when remounting at JET.

The sphere that is the basis for the TOFOR design as described above is specified by its radius (705mm). The center of each S2 detector is placed at $\zeta = 60^{o}$, corresponding to a scattering angle of 30^{o} with a flight path L of 1221 mm giving a flight time of $t_{TOF} \approx 65$ns for neutrons of E_n=2.5□MeV incoming energy.

The instrument consists of a number of different parts and sub-systems. These can be divided in the spectrometer itself (consisting of the S1 and S2 detectors and the mechanical support frame), the system for data acquisition and controls with electronics, and the system to control and monitor (C&M) the pulse response of the TOFOR detectors including calibration stability.

3.1 THE INSTRUMENT FRAME

The TOFOR support frame, made of aluminum, consists of a triangular base plate with three height adjustable floor legs and an upper support ring with three legs attached to the base plate. The base plate and ring function as the chassis for TOFOR. The chassis provides the reference for the physical mounting of the scintillators and their alignment in the TOFOR coordinate system. The origin of the coordinate system (Figure 2) is fixed relative to the center of the base plate whose surface is perpendicular to the system axis.

The base plate has a cylindrical hole of 150.0mm diameter in the center, which is marked by the crossing point of the lines between four holes in the plate. A cylindrical box is placed on top to house the S1 detectors. The S1 scintillators were aligned relative to the base plate and attached to it. The box is covered with a cylindrical lid with a second hole matching the one in the base plate. The only beam-intercepting material, apart from the S1 detector assembly, is a 0.1-mm aluminum foil at the base plate and the box lid acting as light seals.

The S2 support ring is parallel to the base plate, and thus also perpendicular to the system axis. Evenly distributed around the ring are 32 sets of machined holes for steering pins and bolt attachments for the S2 detector holders. The steering pin holes have a tolerance requirement of ±0.1 mm for placing each detector at fixed radius.

3.2 THE S1 DETECTOR ASSEMBLY

The S1 detector assembly is made up of a stack of five detector units. The detectors consist of a circular fast scintillator (Bicron BC-418[1]), with a diameter of 40mm and 5mm thickness (tolerance ±0.05mm). The light emission has a typical rise time of 0.5ns and decay time of 1.4ns. Three light guides (Bicron BC-800) are bonded to the scintillators at 120^{o} angles to each other (Figure 4). These are attached, via optical silicon pads (Bicron BC-634A), to Photomultiplier (PM) tubes. The PM tubes (Electron Tubes 9142A[2]) have a typical transient time jitter of <0.6ns and a gain of 10^{6} at an applied high voltage in the range 945-1145V.

The scintillator and light-guide assemblies are wrapped in a 15mm layer of aluminum foil and separated by black paper to minimize light cross talk when they are placed as a stack in the inner circular enclosure of the S1 box on the base plate (Figure 5). Each detector unit is fixed in position relative to the plate by the light guides, which rest in cradle holders in the inner enclosure wall giving a 1mm clearance between each layer. The lateral scintillator position is determined by clamping one light guide, while the other two are allowed free radial motion due to thermal expansion/ contraction. The detectors were aligned at room temperature (~20^{o}C) relative to the base plate center to within ±0.1mm. The thermal expansion would lead to a radial displacement of the scintillator center <0.01mm/^{o}C in different directions for the 5 layers (expected operating temperatures are 15-35^{o}C).

Each PM tube is mounted in a soft iron pipe, also providing magnetic shielding, whose front cap is clamped to the detector light guide and whose back cap keeps the PM tube in place (Figure 6).

The PM tube is pressed towards the light guide by a spring at the back to assure good optical contact between the PM tube photocathode window, the greased silicone pad and the light guide. The pressure is adjusted with metal rings at the back of the PM tube along with a plastic ring for purpose of electrical isolation. Each PM tube pipe is placed in a cradle attached to the base plate in such a way as to allow longitudinal motion.

Signal cables (with BNC type connectors) and High Voltage (HV) cables from each PM tube, as well as cables from the temperature probes, leave the S1 enclosure through cable feed-through

panels (Figure 5). Each PM tube can be fed with light pulses from the C&M system via optical fibers (Figure 5). Guiding pipes lead the fibers through the inner enclosure to the scintillator side opposite the photocathode of the PM tube aimed at for pulsed light illumination.

Light-tightness of the S1 box was achieved through sealing the base plate and lid joins besides light-tight cable and fiber feed-throughs (Figure 5). The box is ventilated with four fans to remove the heat produced by the PM tubes. Labyrinth ducts in the fans prevent light leaks. The temperature is monitored with three PT100 probes.

3.3 THE S2 DETECTOR ASSEMBLY

The S2 detector is made of 32 modules consisting of a scintillator with attached light guide and PM tube. The plastic scintillators (Bicron BC-420) have light response characteristics in terms of rise/ decay times of 0.5/1.5ns. They are trapezoidal in shape with a thickness of 15.0mm, length of 350†mm and top/base widths of 95.0/134.7mm; the machining tolerance level is ±0.05mm. The geometrical center is used as reference to specify the position of the scintillator within the TOFOR coordinate system. The nominal angular coverage of an S2 scintillator is α-6.98^{o} and α+7.87^{o}. This means, for instance, that 2.5MeV neutrons scattering in S1 have an energy spread from 1.53 to 2.08MeV when they enter S2.

The scintillator base is glued to a light guide (Bicron BC-800) of fish tail shape, which changes from rectangular to circular cross section of constant area (Figure 7). The circular end connects to a PM tube (Electron Tubes D671A) with the characteristics of <0.6ns jitter in the time response and a gain of 5×10^{6} at an applied high voltage within 1830-2230V.

The scintillator-light guide assemblies are wrapped in a 15mm layer of aluminum foil and covered with black cardboard for light-tightness. They are held in position at the light guide that is clamped to the PM tube holder, which is placed in a structure that is mounted on the ring shaped S2 support frame.

The PM tubes are mounted in soft iron holder pipes and kept in place with front and back holders (Figure 8). This arrangement also provides magnetic shielding of the PM tube. Optical contact between the PM tubes and the light guides via greased optical silicone pads is achieved through exerting spring pressure from the back holder.

A plastic ring between the PM tube and the springs provides electrical isolation. Each PM tube in its holder is placed in a support stand (Figure 9) fitted to the S2 ring with steering pins and bolts to match the machined ring holes. The PM tube pipes were aligned relative to a jig so that all S2 scintillator centers ended up on the constant TOF sphere at the specified polar angle of z=2 α = 60.0^{o} and with the desired tilt of 5.0∞.

The tilt was determined through combining calculated flight times for scattered 2.5MeV neutrons from the center of S1 to different positions on S2 with test results for the S2 scintillator light transfer time obtained through characterization of the S2 scintillators with UV LED light (compare [11]); this limited the position dependent spread in recorded flight times to 1ns for 2.5MeV neutrons. The timing results obtained from these UV LED tests on the final S2 scintillators closely match

those from b coincidence tests done on an earlier, 5□mm thick prototype with the same width and height, described in [12].

An optical fiber is directed towards each light guide through a drilled hole in the plastic collar between the soft iron pipe and the light guide (Figure 8). With an angle of 30^{o} to the light guide axis, light can be transmitted to the PM tube photocathode through only one reflection. The individual fibers are connected in a light splitter on the TOFOR chassis with an ingoing fiber from the C&M system. Signal and HV cables from the electronics system are connected directly to each PM tube. Light-tightness of the individual S2 detector modules, for operation in rooms with normal light conditions, was achieved through using o-rings between the PM tubes and the holders, which were sealed with black tape to the plastic collar and the scintillator (Figure 9).

3.4. DATA ACQUISITION ELECTRONICS

The main purpose of the TOFOR Data AcQuisition (DAQ) system is to collect event times with maximum precision and minimal dead-time. The system collects the PM tube signals from the individual S1 and S2 detectors and processes them to obtain the desired information on times t_1 and t_2 and deposited recoil energies E_{p1} and E_{p2} for the S1 and S2 detectors. The recoil energies are needed primarily to ensure that the right events are collected in the timing measurement. They are recorded in the form of pulse height spectra.

Three signal lines of pulse processing can be identified (Figure 10): Line 1 for recording event times on Time Digitizing (TD) boards, line 2 for recording pulse heights via Analogue-to-Digital Converters (ADC) and line 3 for counting events in scalers (Scl).

The front end of the DAQ consists of linear Fan-In-Fan-Out (FIFO) modules of NIM standard with four inputs and four outputs per channel. The signals of the three PM tubes attached to each S1 scintillator are summed in the FIFO, while the 32 S2 detector signals are fed into separate FIFO channels. One FIFO output for each detector is fed into an ADC via a delay, and two outputs are fed into the Logic Circuit (LC) 1, which, in turn, provides signals to the TD (i), and to LC2 (ii and iii) (Figure 10). From LC1, there is also a branch-off leading to the scalers. For S1, the fourth FIFO output is fed to the scalers via another FIFO for a further four-way split to count pulses above four different pulse height thresholds.

In LC1, Constant Fraction Discriminators (CFD) convert the analogue FIFO outputs above high and low threshold levels to logic pulses that are fed into Programmable Logic Units (PLU). The CFD thresholds can be set for different operating scenarios. For instance, for typical data production runs, the signals representing elastic scattering of neutrons in the individual detectors would fall between the two thresholds and the LED pulses from the C&M system above the high threshold. The PLU modules consist of two independent sections with 8 inputs and as many outputs. The sections can be set to give logic outputs for different combinations of input signals. For instance, the PLUs of LC1 receive high and low threshold logic pulses from the CFDs connected to four detectors per section. The PLUs are set to produce output signals for detectors producing signals of

pulse heights passing the low and high thresholds, $V>V_{LOW}$ and $V>V_{HIGH}$, or between the thresholds, $V_{LOW}<V<V_{HIGH}$. Through software selection, signals above the low, between or above the high thresholds can be selected as output (i), i.e., the individual output from each detector. Outputs of types (ii) and (iii) are obtained if any detector within the PLU section produces a signal of a pulse height between the thresholds and above the high level, respectively. Output (i) is the time signal recorded on the TD boards (1) while (ii) and (iii) are inputs to LC2. LC2 is set to produce a trigger to the ADC (2) for the different inputs (ii) and (iii) so as to select detector events of pulse heights within the threshold gate or above either threshold. Specifications for the different electronics modules are listed in Table 1.

The time signals are recorded in the TD signal line (1), using a time stamping technique. Each individual detector signal (i) from the PLUs in LC1 is fed into a separate channel on Time Digitizer (TD) boards. There are 5 boards, each with 8 input channels. The channels have a bin width of 0.4ns and the ability to handle a peak event rate of 1.25GHz or a sustained pulse rate of 5MHz with no dead time [13]. Their storage capability is 8 MEvents. The five TD boards, residing in two PCs, are synchronized during the initialization phase for each JET discharge. Three channels on one of the boards (Figure 10) receive clock pulses from the central JET computer system in the form of one 1 Hz signal, one 1kHz signal and a single 'pre' signal sent when the acquisition starts for each JET discharge. All events are recorded relative to the 'pre' signal to match the clock time of the TOFOR DAQ to that of JET, which is used to describe the time evolution of plasmas (see section 4). The TD boards record 5 S1 and 32 S2 time trains of individual detector events, from which 160 flight time spectra for all possible S1-S2 combinations can be obtained. These are, in turn, used to construct t_{TOF} spectra, which are then analyzed to obtain the desired information on the energy distribution of the incoming neutron flux.

Analogue signals from all detectors are sent along line 2 to the ADCs, which are triggered by logic pulses from LC2 via the histogram memory units. The digitized ADC outputs are fed into the histogram memory units for storage of data in the form of pulse height spectra. The event rates in the detectors, especially S1, during plasma discharges can be very high leading to significant dead time in the corresponding ADC. This is partially controlled with the help of the triggering options offered by LC2 so as to record pulse height spectra for regions of particular interest. It should be noted that a principal function of the pulse height spectral information is to determine the energy span of neutron generated proton recoils that were selected by the threshold gates defined by LC1 [14].

The scaler line (3) serves two functions, where the first (3a) is simply to record the count rate above the low CFD threshold from LC1 for each individual detector. A level translator before the scaler provides the needed conversion from NIM to ECL signal format. The readout interval for the scalers during the acquisition period can be varied to record the data with the time resolution that suits the situation.

Scaler line 3b is used only for the five S1 detectors. The function is to monitor the PM tube gain

stability during JET discharges to determine the effect of high count rates on the PM tube signal. A second set of FIFO modules is used to split the original summed S1 FIFO output signals for each S1 detector in four, which are fed into CAMAC discriminator channels with different threshold settings. The thresholds are set so that the C&M system light pulses fall in the center of the pulse height interval created. In this way, a change in pulse height due to a PM tube gain shift will be reflected in a variation in the ratio between count rate of events above different threshold levels.

The TOFOR DAQ system is linked to the JET COntrol and Data Acquisition System (CODAS) [15], which provides trigger signals to the DAQ and the clock input to the TDs. This is further described in section 4.

The DAQ system is housed in three cubicles on the second floor of the JET roof laboratory. Signals from TOFOR reach the cubicles through RG 58 cables of 30 m length. The TOFOR PM tubes operate on High Voltage (HV) supplied by a HV power supply located in the electronics cubicles and controlled via the DAQ computers. The installed PT100 temperature probes (3 in the S1 box, 2 on the S2 detector ring and 3 in the electronics cubicles) are read out by PT104 read-out units[3], which are connected to the DAQ system in the electronics cubicles.

3.5 THE C&M SYSTEM

The TOFOR C&M system [16] was designed based on the one used on the MPR spectrometer [17]. It was developed to serve also the MPR upgrade (MPRu) [18]. It consists of two Pulsed Light Sources (PLS). One is a laser emitting 0.65-ns pulses of green light (l=531 nm) at a frequency f~5 kHz, whose intensity can be varied through the use of a polarizerThe same laser is used for both the TOFOR and the MPRu systems. The other PLS is an LED emitting blue light ($\lambda = 428$ nm). It is energized with a driver developed for TOFOR producing 8-ns pulses of selectable frequency, typically set at 5kHz [19]. The PLS are placed in a separate cubicle in the roof laboratory with fiber optics runs to the TOFOR spectrometer and cable runs to the DAQ system [20]. The C&M outgoing fiber ($\phi = 3.0$mm) is split into a bundle of 57 individual 250μm fibers out of which 47 are individually connected to each TOFOR PM tube. Light pulses issued from the laser or the LED reach all detectors simultaneously (within 0.1 ns as given by the mechanical tolerance of the fiber construction).

As a calibration and stability reference for the PLS, one fiber is used to illuminate a PM tube of S1 type fitted with a small scintillator in which signals of constant pulse height are produced with a ^{241}Am α source (~3 kBq in 2005).The PLS are monitored for intensity drifts using this ^{241}Am absolute reference detector. The laser is typically stable to within 5% over a 1 h period and the LED to within <0.5% over a 15 h period [16].

A ^{22}Na source (~450Bq in February 2005) is placed near the S1 scintillator stack in the central enclosure (Figure 11) to allow for collection of reference pulse height spectra with distinct Compton edges, corresponding to its 511keV and 1274.5keV γ-lines. This information is used in order to relate the discriminator threshold settings in mV to pulse heights.

3.6 NEUTRON TRANSPORT MODEL OF TOFOR

As mentioned in section 2, the TOFOR design was based on the results of extensive Monte Carlo neutron transport simulations [9]. The simulations were also used for performance evaluation, as an analysis tool and to create a detailed response function for the instrument [14].

The simulation model of the TOFOR spectrometer was created to include the scintillators themselves and other relevant components with regard to composition and geometry that have an effect on the neutron transport in the instrument. Neutron transport calculations were used to simulate the distributions of the times t_1 and t_2, and the deposited proton recoil energies, E_{p1} and E_{p2}, i.e., the characterizing parameters of neutron events in the individual detector elements for a given incoming neutron energy, E_n. In particular, it was determined which of the events in S1 and S2 belonged to the same neutron.

With the model, the pure geometrical response of the instrument to incoming neutron fluxes of different energies over the range of interest, typically, E_n=1 to 5MeV, could be simulated. Multiple interactions in the scintillators or the surrounding structural materials as well as scattering on carbon in the scintillators themselves were in this way accounted for in addition to the single scattering events on hydrogen in S1 and S2. The resulting t_{TOF} distributions were used to create the geometrical neutron response matrix $R_n(E_n, t_{TOF})$. A graphical representation of R_n is given in Figure 12, where the interval E_n=1 to 7MeV is covered with a step length of 50keV in the simulations and low and high threshold levels set to correspond to proton recoil energies of 0.32 and 2.30MeV for S1 and 0.54 and 2.58MeV for S2, respectively.

The total response $R(E_n, t_{TOF})$ includes R_n but also the pulse response R_p, which describes how the neutron parameters t and E_p manifest themselves in the measurement including light production, signal processing in the electronics, etc. Input to R_p comes partly from measurement of the area response variation of the scintillators with respect to timing and pulse height response for a certain amount of deposited energy as derived from measurements with ionizing radiation sources as well as a UV LED PLS [11]. It can be noted that R_n can be considered as the fundamental one with which R_p is folded in terms of some approximate function expressing the intrinsic (pulse) resolution for the time measurement as is further discussed in section 5.

4. INSTALLATION AT JET AND OPERATION

TOFOR was reassembled in the JET roof laboratory in February 2005 above a 1.90m long collimator (diameter of 40.7±0.2 mm) with respect to which it was aligned (Figure 13). The alignment was performed with the help of a photogrammetry survey [21,22] so that the TOFOR system axis was parallel with the collimator axis (that is tilted 0.935∞ from the plumb line) to within 0.016°. The center of the S1 plate was measured to be -0.75/+0.09mm away from the collimator center in the lateral x/y directions, i.e., a total radial shift of 0.76mm. Considering the collimator geometry, this means that the entire S1 scintillator is within the collimated neutron flux. The S2 ring was surveyed to have center coordinates 2.10/-0.24mm [21] at a height of 550mm from the base plate. The survey

results show that the positioning of the instrument is well within the requirements so as to have no practical impact on the extraction of the energy distribution of the incoming flux from measured t_{TOF} spectra.

The TOFOR sight line through the JET plasma is defined by the collimator through the roof laboratory floor (Figure 14). It gives a cross section for the maximum area of plasma viewable of 3700cm^2 at the tokamak mid-plane at a distance of 19m from the roof laboratory floor. However, this sight line is curtailed in the toroidal direction by the vertical diagnostic port on the vessel. In the radial direction, the collimator view is 40cm wide, to be compared with the plasma minor radius of 1.2m. Above the vertical diagnostic port, there is a pre-collimator consisting of two pairs of jaws that are movable in the radial[4] and toroidal directions and that can thus be used to limit the viewed plasma volume. On their way from the plasma to TOFOR, the neutrons pass through a 7mm thick steel plate at the port, 16†m of air, two old sets of thin metal wires in the torus hall ceiling and a 1-mm aluminum foil at the collimator base serving as gas separator between the torus hall and the roof laboratory. The flux leaving the collimator has a divergence of 10.5mrad, which has negligible effect on the cross section of the neutron beam through TOFOR compared to a parallel one. The parallel beam approximation was used in the TOFOR response simulations.

TOFOR is designed for observation of the collimated neutron flux (F_n) from JET deuterium plasmas. The JET plasmas are maintained over time periods of up to 100 s with a preparation time of typically 30 minutes to launch the next. Experimental campaigns extend over periods of months. The plasma conditions can vary in time, spontaneously or by external controls, manifesting themselves in both yield rate and energy distribution of the neutron emission. The expected yield rates fall in the range between $Y_n^{MIN} \leq 10^{12}$ n/s and $Y_n^{MAX} \approx 10^{17}$ n/s, corresponding to collimated neutron fluxes between $F_n^{MIN} \leq 4\times10^{1}$ n/s$\cdot$cm^2 and $F_n^{MAX} \approx 4\times10^{6}$□n/scm^2. Basic plasma conditions produced with Ohmic heating will have a yield rate below $Y_n \approx 10^{13}$□n/s. High rate plasmas are produced with the help of auxiliary heating. The TOFOR count rate response is C_n = 4kHz for $Y_n \approx 10^{15}$ n/s. Since ~4×10^3 counts is deemed sufficient for detailed analysis, this means that time resolved t_{TOF} spectra of good quality can be collected for plasmas of $Y_n \geq 10^{15}$ n/s, while the study of Ohmic plasmas require long time integration periods or even summation of similar discharges to obtain desired statistics. The high-count rate achievable for high yield rates affords improvement of the time resolution in the analysis, which is needed to study the fast transients that occur in plasmas with auxiliary heating. Typical for the observation conditions at JET is that the yield rate, and hence the count rate, undergo large variations over a discharge including significant transients of different kinds.

Before plasma operation starts, TOFOR is set to certain working points, e.g., through tuning of the discriminator thresholds in LC1 (see section 3.4). The lower threshold is rather critical (especially for S1) since it affects the admixture of multiple scattering events in the recorded t_{TOF} spectra. The TOFOR response function requires knowledge of threshold levels in units of recoil proton energy (E_p in MeV), or equivalent pulse height recoil electron energy (E_e in MeVee), while threshold levels are set in mV for pulse height. The relationship between PM tube pulse height and the

corresponding recoil electron energy E_e for the individual detectors is determined by recording ^{22}Na pulse height spectra. For TOFOR, it was determined that the most convenient way of assuring accurate settings of all threshold levels was setting all low discriminator thresholds to the same value (typically 30mV) and subsequently tuning the PM tube gains so that the same background count rates are obtained in all S1 and all S2 detectors, respectively. The gain level is then chosen so that the pulse height corresponds to accepting recoil protons over a set energy. Accurate setting of the thresholds is especially important for the three PM tubes on each S1 scintillator, which are summed to form a single pulse.

Another important point is the time alignment of the individual S1 and S2 detectors so that signals t_1 and t_2 recorded by the TD boards can be used to construct t_{TOF} spectra. For this purpose, LED pulses from the C&M system and a CAMAC TDC module with 50ps time resolution were used. Adjustments were made with delay cables to align within 0.1 ns. This allows for addition of the individual t_{TOF} spectra without further corrections.

After TOFOR has been set up for data taking, the C&M system is used to monitor the stability of the working points. This is done with respect to drifts between plasma discharges as well as over full experimental campaigns. The discriminator threshold settings are monitored with laser pulses of variable intensity. The long-term stability is checked through analysis of PLS generated pulse height spectra for each individual detector. Monitoring of the transient gain stability of the S1 detectors during discharges is performed with LED pulses using the ratios of count rates above different threshold levels. Monitoring of the timing stability is done by collecting time spectra generated by PLS or cosmic muons or ambient gamma radiation recorded over long time periods (nights) in order to achieve good statistics.

The running of TOFOR includes communication between the DAQ system (section 3.4) and the JET CODAS system. Prior to each plasma discharge, CODAS sends an HTTP request to initialize the data acquisition (Figure 15). This signal triggers the synchronization of the TD boards, which start collecting data as soon as the synchronization is finished. About two minutes after the initialization, the JET discharge countdown is begun via a pre-signal, which is given both as a trigger signal and as an HTTP request. The HTTP request starts the CAMAC subsystems and triggers the C&M system. The trigger signal is recorded in one of the TD channels (‘clock’ in Figure 10) providing synchronization between the TOFOR DAQ system and the central JET clock. CODAS also sends two clock signals with frequencies of 1Hz and 1kHz, which are fed into the TD boards serving as the time calibration of the boards.

The plasma discharge starts 40s after the pre-signal and an end-of-pulse HTTP request is sent after its completion, which triggers the data transfer from all the data acquisition devices to local PC storage. At some later time CODAS sends a request for the data, which is then transferred. If all data is successfully received by CODAS then a data archived signal is sent to the local PC and the discharge is closed. Otherwise a new HTTP request for transfer is sent.

In order to record data not connected to JET operation, TOFOR can be triggered locally. For

instance, spectra from radioactive sources, ambient background radiation or C&M system signals can be recorded in this way. This feature is used for C&M functions not implemented to be performed as part of each JET discharge.

DISCUSSION

The aim set for TOFOR was to exploit fully the high flux from JET deuterium plasmas and translate it into high-count rate (C_n). To this end, the count rate capability (C_n^{CAP}) should be sufficient to allow operation of TOFOR up to the maximum JET neutron flux, while TOFOR should be capable of operating over the full dynamic range $D=F_n^{MAX}/F_n^{MIN} = 4 \times 10^6/4 \times 10^1 = 10^5$ discussed in section 4 if sufficient integration time is allowed. The efficiency required to reach these count rates should be balanced against a desired energy resolution of order 7% FWHM. Moreover, plasmas produce neutrons with a significant energy spread (typically 1 to >5MeV), which requires a spectrometer with matching bandwidth.

The performance depends on the hardware and here we shall highlight its functionality for its intended purpose. On the one hand, the volumes of the S1 and S2 scintillators need to be large to reach high flux detection efficiency and, hence, count rate; this also means that S2 should provide maximum coverage of the solid angle for neutrons scattered from S1. On the other hand, the volumes must be limited to avoid too high admixture of multiple scattering events in the measured t_{TOF} spectrum relative to those due to neutrons that only scattered once in S1 and once in S2. The resolution $\Delta t_{TOF}/t_{TOF}$ of the measured t_{TOF} spectrum for a mono-energetic neutron flux can be expressed in terms of an energy resolution $\Delta E_n/E_n$, where that for E_n = 2.5MeV can be taken as representative for TOFOR performance. A volume limit was also set by the required t_{TOF} resolution for given E_n belonging to the neutron response function R_n. From the optimization simulations with the GEANT4 code, it has been determined that the flight path variations relative to the constant TOF sphere geometry (Figure 2) would contribute $[\Delta E_n/E_n]_{Rn}$=5.8 % to the energy resolution for 2.5MeV neutrons with a flux efficiency value of ε = 0.12cm^2 [9]. This is the instrumental resolution that one would observe for mono-energetic neutrons of E_n=2.5 MeV apart from the finite resolution by which the times t_1 and t_2 for events in S1 and S2 can be measured, i.e., $[\Delta E_n/E_n]_{Rp}$. Although R_p is complex it can, to lowest order, be assumed to be independent of E_p [23]. When represented with a Gaussian distribution, a value of $[\Delta t_{TOF}]_{Rp}$=1.5ns (FWHM) has been estimated based on preliminary measurements at JET [24]. An intrinsic time resolution of 1.5ns gives a contribution of 2 × (1.5/65) = 4.6% to the total energy resolution $\Delta E_n/E_n$=7.4 % (FWHM). This approximation has been used for R_p, as part of R, to describe and analyze the measured t_{TOF} spectra in experiments at JET to illustrate the TOFOR performance. The resolution should be compared to the set target of ~7%.

A central aspect for the performance is count rate capability, C_n^{CAP}. This depends on the acceptable upper limit on the ratio between accidental events and true coincidences in the selected region of the measured t_{TOF} spectrum, i.e., the ratio C_x/C_n. The accidental event rate is directly related to the single rates in S1 and S2, i.e., $C_x = C_1 \times C_2 Dt_C$, where Dt_C is the selected time region. The random

level can be controlled and reduced by accepting only desired events, for instance, through pulse height discrimination. This is most effectively applied to C_1. In TOFOR, it is done by eliminating events that are kinematically incompatible with *np* scattering into S2. As all count rates increase with the incoming neutron flux, i.e., $C_x \propto F_n^2$ and $C_n \propto F_n$, one obtains $C_x/C_n \propto F_n$. In other words, the random contribution increases linearly with the flux, meaning that weak contributions to the spectrum will be harder to distinguish at higher count rates. C_n^{CAP} is also limited by the fact that the single rates must not exceed the rate limit of individual PM tubes. The single rates in S2 are lower so this is most critical for the in-beam detector, S1, which is therefore split into five scintillator units to improve its performance at high rates [9]. Both the single rate and the C_x/C_n limitations are closely related to the capabilities of the DAQ system.

The data of recorded events in the t_1 and t_2 time traces are checked for pairs within a certain time region of the t_{TOF} spectrum $\Delta t_C = \Delta t_- + \Delta t_+$ as defined above, such that for every S2 event time t_2 the S1 coincidences fall in $t_2 - \Delta t_- \le t_1 \le t_2 + \Delta t_+$, where $\Delta t_{-/+}$ can be chosen arbitrarily. These time pairs can be analyzed over sequential time intervals of a discharge (typically tens of milliseconds and upwards) to construct the t_{TOF} spectrum. This spectrum contains both accidental and true neutron coincidence pairs of S1 and S2 events, with the true ones concentrated to regions populated by fusion neutrons of say $E_n < 7$MeV, i.e., $t_{TOF} > 38$ns. Negative flight times (S2→S1) can be recorded with TOFOR as easily as positive ones due to the time stamping technique of the TD boards.

The level of random events per spectral channel, c_x, is constant across the t_{TOF} spectrum and can be determined based on data in the region from $t_{TOF} \approx -10$ns down to $t_{TOF} = -200$ns. Thus, the c_x level is the measured average over some 500 channels providing a high accuracy in the value subtracted from the measured t_{TOF} spectrum to obtain a reduced spectrum representing the true coincidence rate per channel, i.e., $c_n = c_m - c_x$, where c_m is the measured event rate per channel. This also implies that the variation in the random event rate over time can be determined on a shorter (<10 ms) scale than that of the plasma time interval $\hat{\imath}t_P$ which is typically >100 ms for acquired data based on $c_n(t)$.

The stability of the TOFOR time-of-flight spectrum is regularly monitored with the integrated C&M system. The time scale of the spectrum is given by a zero point (determined through recording of LED pulses) combined with the TD board bin width of 0.4 ns. The contribution to the uncertainty from the bin width is found to be negligible when double-checking against the JET clock pulses. The zero-point contribution is ~0.4 ns. This leads to an indetermination in the derived neutron energy spectrum due to the calibration of the time spectrum on the single percent level for 2.5MeV neutrons.

To illustrate the TOFOR performance, we study a t_{TOF} spectrum recorded for a plasma producing a high neutron flux. This was achieved in the deuterium Pulse No: 69093 that was heated with neutral beams (NB) of deuterium atoms as well as radio frequency power (RF) tuned to the second harmonic resonance frequency of deuterons. The injected power was $P_{NB} = 22$MW, with beam energies of $E_b = 80$ and 130keV, and $P_{RF} = 6$MW, giving a neutron yield rate of $Y_n = 1 \times 10^{16}$ n/s.

The spectrum shown in Figure 16a is based on data accumulated during the plasma time interval t_P = 6.0-8.5s (i.e., Δt_P = 2.5s) of the discharge. At $t_{TOF} \approx$ 4ns, there is a small peak due to gammas (in the few MeV range) in the beam from the plasma, which scatter in S1 and arrive 4.1ns later in S2. This gamma peak provides a consistency check for the TOFOR time calibration.

The broad spectrum from $t_{TOF} \approx$ 50ns and upwards is due to true neutron coincidences while the region with 10ns < t_{TOF} < 40ns is dominated by random events. The average random level is determined from the time interval −200ns < t_{TOF} < −10ns as described above. One obtains a value of n_x = 160 counts per channel, corresponding to a random rate of $c_x = n_x/\Delta t_P$ = 64Hz per channel. After subtraction of the random events, a reduced t_{TOF} spectrum as shown in Figure 16b is obtained. The subtraction of n_x eliminates the events in the t_{TOF} <40 ns region apart from the gamma peak and the statistical scatter.

The coincidence count rate in the reduced spectrum is C_n = 39kHz within the selected time-of-flight window, 0 ns ≤ t_{TOF} ≤ 200ns. The spectrum is dominated by the peak at $t_{TOF} \approx$ 65ns, which corresponds to single scattering neutron events of energies $E_n \approx$ 2.5MeV, while multiple scattering events give a tail towards higher t_{TOF}.

The peak count rate in the t_{TOF} spectrum in Figure 16b occurs at $t_{TOF} \approx$ 65ns from which one derives c_n = 1.6kHz. The random-to-true ratio is thus c_x/c_n=4.2% in the peak channel. For the chosen integration time Δt_P, the subtraction of the random events increases the statistical uncertainty in this channel from 1.58% to 1.65%. It is interesting to project the effect of the random admixture and subtraction towards higher neutron fluxes F_n. For JET, the maximum 2.5MeV neutron yield rate is estimated to be $Y_n \approx 10^{17}$ n/s, giving a neutron flux and thereby a count rate about 10 times higher than in Pulse No: 69093, i.e., $C_n \approx$ 400kHz . The random level increases to c_x/c_n = 43%, but the higher flux results in better statistics; for a data collection time of 2.5s the statistical uncertainty is 0.42% before and 0.60% after background subtraction. However, the higher neutron flux does not allow for correspondingly shorter data collection times; Δt_P = 0.25s results in statistical uncertainties of 1.33% without but 1.90% with background subtraction. Thus, the total number of counts required for a certain statistical accuracy increases with the count rate.

Calculations indicate that spectroscopy of components on the few percent level is possible for count rates of about 40kHz with a time resolution of Δt_P = 2.5s. For weaker components, the neutron flux has to be decreased and longer data collection times are required. On the other hand, the main peak can be analyzed at count rates of C_n = 400kHz with a time resolution of Δt_P = 0.25s and a statistical accuracy better than 2%.

To be able to deduce the spectral broadening and thus the plasma ion temperature, c_x/c_n at half the peak amplitude should not exceed 1:1. From these numbers, an upper limit for the TOFOR count rate capability of C_n^{CAP} = 500kHz is deduced. At this count rate level, the single rates in the individual S1 layers also approach their capability limit.

The TOFOR measurements can also be illustrated in terms of count rates as functions of plasma time t_P. The single rates of the S1 and S2 detectors, $C_1(t_P)$ and $C_2(t_P)$, are presented in Figure 17.

Here, one can note that $C_1(t_P)$ for S1 starts at a low level in the 50Hz range up to $t_P \approx 44.5$s, reflecting the plasma conditions with Ohmic heating only, which it returns to for $t_P > 52$s. The intermediate region of higher rates, with a plateau at the 1 MHz level from $t_P = 45$ to 52s, is due to enhanced neutron yield rate caused by the application of auxiliary heating. The time trace $C_2(t_P)$ for S2 shows the same general trend, but for a higher constant rate level before and after the heating period. This is due to ambient background radiation to which S2 has a higher sensitivity than S1 in proportion to its greater scintillator volume (a factor of 10^3). Since $C_x \mu C_1 C_2$, the amplitude swings seen in Figure 17 will be further amplified in the random rate $C_x(t_P)$.

Below, some examples illustrating how the measured t_{TOF} spectra are used to extract information on the energy distribution of the incoming neutron flux are given. The first example is JET discharge Pulse No: 68396, a NB heated deuterium plasma with a power of $P_{NB} = 7.0$MW injected with 130-keV beams. The NB power creates a neutron source of a quasi-steady state lasting about 9s at a yield rate of $Y_n = 1.5 \times 10^{15}$ n/s resulting in a TOFOR count rate at the $C_n = 6.3$kHz level. The measured t_{TOF} spectrum (integrated from 4.5 to 13.5s of the plasma discharge) was determined to have an average accidental admixture of n_x=14 counts per channel which was subtracted to obtain the reduced t_{TOF} spectrum (Figure 18).

This spectrum was compared with the predicted t_{TOF} distributions obtained from an assumed incident neutron spectrum $F_n(E_n)$ folded with the response function—$R(E_n, t_{TOF})$. From the parameterized model for—$F_n(E_n)$, one produces a trial spectrum, consisting of a thermal and a beam neutron component, which is varied to give the best fit to the measured t_{TOF} spectrum with the result presented in Figure 19. The thermal component is modeled with a Gaussian and the beam component using a half-box slowing down distribution; for further details concerning the modeling see [24]. The shape of $F_n(E_n)$ is fairly well established in this case so the achieved good description of the data lends credit to the instrumental performance and the adequacy of the matrix R of TOFOR. With regard to the latter it is especially noteworthy that the sloped t_{TOF}<62 ns region of the t_{TOF} spectrum (Figure 18), which is the high-energy (E_n>2.5MeV) side of the neutron spectrum, is well accounted for over more than two orders of magnitude. The structure on the low energy side could be explained by finer details in the instrumental neutron scattering characteristics currently in the process of being implemented in the response function.

Another example is Pulse No: 69529 subjected to Radio Frequency (RF) heating, specifically, ion cyclotron resonance heating coupling to the second harmonic frequency of deuterons in the plasma center. The effect is typically their acceleration to high energies, i.e., temperatures of the order 100keV compared to the bulk deuterons of a few keV. The high-energy deuterons produce neutrons with a large energy spread when they fuse with bulk deuterons. The result is a t_{TOF} spectrum (Figure 20, integrated from 10 to 20 s of the plasma discharge) that is much wider than that for NB injection (Figure 18). It can be well described with a predicted t_{TOF} spectrum using the neutron spectrum shown in Figure 21, with a thermal and an RF neutron component. Again, the model used for the thermal component is a Gaussian. The RF component is modeled based on a perpendicular

Maxwellian deuterium distribution (see [24]).

In this case, the neutron spectrum is found to have a significant amplitude over an extended energy range from about E_n=1.7 to 4MeV. The region of interest in the t_{TOF} data ranges from below $t_{TOF} \approx 50$ to about 80ns (Figure 20). The observation of RF heated plasmas is, therefore, a test of TOFOR as a broadband neutron spectrometer.

The principal neutron source situations that TOFOR will meet at JET are summarized in Table 2 along with the type of Neutron Emission Spectroscopy (NES) diagnostic information one can expect to obtain. The source characterization is based on intensity, i.e., the neutron yield rate Y_n, and the resulting average count rate, C_n, in TOFOR. The source is also characterized by the energy range around 2.5MeV that is of interest requiring spectrometer energy bandwidth capability to cover it. Three classes of experiments are listed based on how the velocity distribution of the deuteron population is changed by external means as compared to the base condition of a thermal equilibrium plasma produced using Ohmic heating only.

The plasmas of the first type, with Ohmic heating only, would be a source of low intensity that emits neutrons with an energy distribution of Gaussian shape whose width is determined by the deuteron temperature, typically, a few keV, and hence an energy spread ~5% (FWHM). Neutral beam heated plasmas have deuteron velocity components up to the beam energy and produce neutron spectra with a width of up to 15 %. The source strength is now considerably increased; yield rates up to the $Y_n \approx 10^{16}$ n/s range have been produced at JET during the operating period since 2006 that TOFOR has been in use. With NB heating in combination with RF one could reach a maximum in the $Y_n = 10^{17}$ n/s range and, hence, count rates of up to 0.5MHz. RF has a strong effect on the deuteron population with high velocity tails, equivalent to ion temperatures up to 500keV, as a particular signature. To measure these one needs a neutron energy bandwidth of about 100%, but the neutron yield rate and, hence, count rate is lower than when only NB is used. Finally, deuteron velocity tails can also be produced in plasmas if fast ions, such as produced with RF, suffer head-on collisions with bulk deuterons [4]. These are referred to as knock-on collisions and can produce neutrons of even higher energies than for RF heated plasmas requiring a correspondingly greater spectrometer bandwidth [25]. During the operation period since the beginning of 2006, the TOFOR spectrometer has been used in all these types of experiments.

CONCLUSIONS

TOFOR is a spectrometer to perform advanced Neutron Emission Spectroscopy (NES) diagnosis of deuterium plasmas in magnetic confinement. The instrument implements the two scintillator detector systems S1 and S2, with the latter covering a large area of a sphere which allows the energy distribution of the incoming neutron flux to be determined from the measured flight time (t_{TOF}) distribution. A C&M system with new pulsed light sources is implemented to assist in the calibration and verification of the instrumental stability. The times of events in S1 and S2 are measured with dedicated PC cards that allow continuous recording and storage of data for entire

JET discharges lasting up to tens of seconds. The spectrometer response to neutrons was modeled to determine the t_{TOF} spectrum for arbitrary energies in the typical range 1 to 5 MeV, or higher with reduced sensitivity. The response simulations give a detailed description of the single and multiple scattering contributions to the t_{TOF} spectrum, which is the basis for extracting information on the incoming neutron spectrum.

The performance of TOFOR has been demonstrated in measurements at JET. While TOFOR is optimized for neutrons around 2.5MeV, good NES results have been extracted for a bandwidth from 1 to >5MeV. TOFOR has been operated successfully at count rates up to 40kHz when JET operated at a yield rate of 1/10 of its expected maximum of Y_n=10^{17} n/s. The results obtained indicate a count rate capability limit of about 0.5MHz which could be approached in future JET experiments. The data taken with TOFOR at JET show that the t_{TOF} spectra recorded for different neutron emission conditions are described by the response function and the analysis model. Thus, the results obtained from the analysis is taken as a demonstration of the level of confidence that can be placed in the NES diagnostic results.

TOFOR, with the new data acquisition, has demonstrated great versatility as exemplified by the measurement of the t_{TOF} neutron spectra for different plasma conditions at JET. Moreover, it also allows one to reduce the admixture of accidentals in the measurement besides making accurate correction thereof. The new data acquisition system has contributed to raising the count rate capability of TOF instruments in NES diagnosis of fusion plasmas by more than an order of magnitude.
With the TOFOR instrument it is now possible to perform NES diagnosis of deuterium plasmas with considerably higher quality of data than has been previously possible. The target set for TOFOR to reach the same NES diagnostic capability for D plasmas that has been previously demonstrated by other types of instruments for DT plasmas has been achieved.

ACKNOWLEDGEMENTS

This work has been performed under auspices of the European Fusion Development Agreement and the Association EURATOM-VR (Sweden). It has been financially supported as the JET Enhancement project on contract EFDA JET/CSU# JW1-EP-DIAG.TOFOR, the Swedish Research council (VR), Uppsala University, Milano-Bicocca University, and Institute of Plasma physics (CNR), Milano.

REFERENCES

[1]. G. Ericsson et al., Rev. Sci. Inst. **72** (2001) 759-766.
[2]. T. Elevant, Nucl. Instr. Meth. A **476** (2002) 485-489.
[3]. O.N. Jarvis, Nucl. Instr. Meth. A **476** (2002) 474-484.
[4]. L. Ballabio et al., Phys. Rev. Letters **85** 6 (2000) 1246-1249.
[5]. G. Gorini and J. Källne, Rev. Sci. Instr. **63** 10 (1992) 4548-4550.
[6]. A. Hjalmarsson et al., Rev. Sci. Inst. **72** (2001) 841-844.
[7]. A. Hjalmarsson et al., Rev. Sci. Inst. **74** (2003) 1750-1752.

[8]. L. Ballabio et al., Nuclear Fusion, Vol. **38**, No. 11 (1998).
[9]. A. Hjalmarsson et al., "Neutron transport simulations for the design and performance optimization of the TOFOR neutron time-of-flight spectrometer", UU-NF 05#12 Uppsala University, Neutron Physics Report ISSN 1401-6269 (December 2005) to be published.
[10]. S. Agostinelli et al., Nucl. Instr. Meth. A 506 (2003) 250-303.
[11]. A. Hjalmarsson et al., "Characterization of a scintillator detector with charged particles and pulse light emission", UU-NF 05#13 Uppsala University, Neutron Physics Report ISSN 1401-6269 (December 2005), to be published.
[12]. L. Giacomelli, "Development of Instrumentation for Neutron Emission Spectroscopy Diagnosis of Fusion Plasmas in Deuterium", Uppsala University Neutron Physics Report UU-NF 02#9, ISSN 1401-6269 (July 2002).
[13]. J. Sousa et al., Fusion Eng. Des. **71** (2004) 101-106.
[14]. A. Hjalmarsson et al., "Response function simulation of the TOFOR neutron time-of-flight spectrometer", UU-NF 06#06 Uppsala University, Neutron Physics Report ISSN 1401-6269 (December 2005), to be published.
[15]. C. Hogben and S. Griph, Interfacing to JET Plant Equipment Using the HTTP Protocol, CODAS Document Centre, http://w3.jet.efda.org/CODAS/Document_Library (2002).
[16]. M. Tardocchi et al., Rev. Sci. Instr. **75** 10 (2004) 3543-3546.
17]. M. Tardocchi et al., "The Monitoring System of the MPR Focal Plane Detector", UU-NF 00#3 Uppsala University, Neutron Physics Report ISSN 1401-6269 (February 2000).
[18]. G. Ericsson et al., "Upgrade of the Magnetic Proton Recoil (MPRu) Spectrometer for 1.5-18 MeV neutrons for JET and the next step", Proceedings of Science PoS (FNDA 2006) 039 (2006).
[19]. E. Ronchi, "A Bipolar LED drive technique for high performance, stability and power in the nanosecond time scale", to be published.
[20]. JET Final Report JW2-OEP-ENEA-21.01, Responsible Officer G.Gorini.
[21]. JET site inspection report JET6678, Alstec systems technology, 02.03.2005.
[22]. JET site inspection report JET6677, Alstec systems technology, 02.03.2005.
[23]. A. Hjalmarsson, "Development and construction of a 2.5MeV neutron time-of-flight spectrometer optimized rate (TOFOR)", Ph.D. thesis Acta Universitatis Upsaliensis no 233 from Faculty of Science and Technology, Uppsala University (2006).
[24]. C. Hellesen et al., "Measurement and analysis of the neutron emission from ICRH and NB heated JET D plasmas using the TOFOR spectrometer", to be published.
[25]. L. Giacomelli et al., "Neutron Emission Spectroscopy Diagnosis of Fast Ions in RF D(^{3}He) Heated Plasmas at JET", UU-NF 07#10 Uppsala University, Neutron Physics Report ISSN 1401-6269 (June 2007).

NOTES

[1] Manufactured by Saint-Gobain Crystals … Detectors, Newbury, Ohio, USA.
[2] Manufactured by Electron Tubes Limited, Ruislip, UK.
[3] Manufactured by Pico Technology Limited, St Neots, UK.
[4] The jaws should allow radial scan of the viewed plasma volume but this was only partially possible at the time of installation.

Line	Module	Acronym	# of units	Manufacturer/ Model
Common	Linear Fan-In-Fan-Out	Lin FIFO	10	Caen N401, N625
Common	Constant Fraction Discriminator	CFD	10	Ortec CF8000
Common	Programmable Logic Unit	PLU	6	Caen C542
1	Time Digitizing Board	TD	5	IST (PCI type)
2	Logic Fan-In-Fan-Out Log	FIFO	3	Caen N454
2	Analog-to-Digital Converter	ADC	3	LeCroy 4300B FERA
2	Histogram Memory	Hist Mem	3	LeCroy HM413
3	Linear Fan-In-Fan-Out Lin	FIFO	2	Philips PS748
3	Discriminator, Level Translator	Disc, LT	2	Caen C207
3	Scaler	SCL	2	LeCroy 4433 (ECL)
N/A	High Voltage power supply		1	Caen SY2527
N/A	HV supply board		4	Caen A1733N

Table 1: List of electronics modules used in the TOFOR electronics setup.

Plasma type	Neutron source		TOFOR response
	Y_n range (n/s)	E_n spread (FWHM)	C_n (kHz)
Ohmic	$<10^{13}$	5%	<0.04
NB (E_d=130 keV)	$<10^{16}$	15%	<40
RF (T≈500 keV tails)	$<10^{15}$	100 %	<4
Knock-on		>100 %	~0.5

Table 2 : Examples of JET plasma types with the corresponding neutron source conditions generated and the approximate TOFOR count rate response.

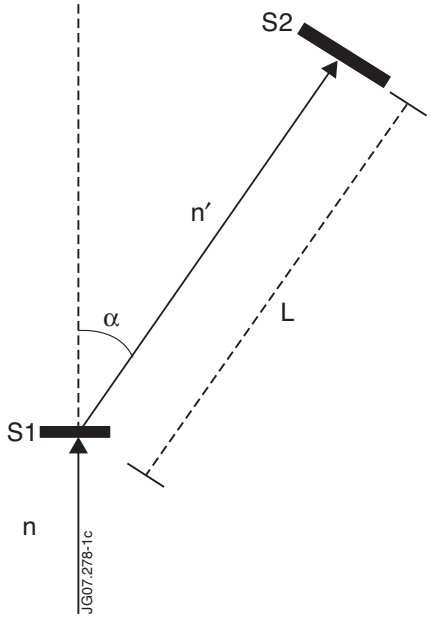

Figure 1: Definition of the neutron flight path in a TOF system. The incident neutron n scatters in the S1 detector through the angle α and the scattered neutron n' goes on to be detected in the S2 detector. L is the distance S1-S2.

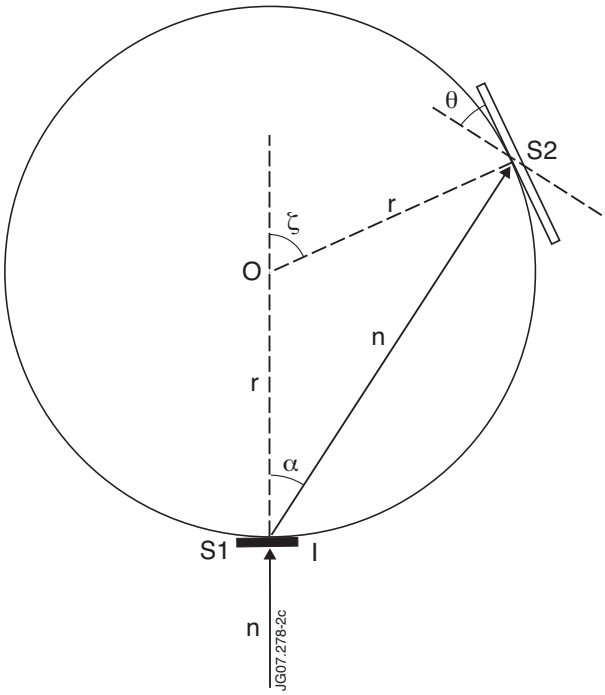

Figure 2: Definition of the TOFOR coordinate system and sphere of constant TOF with origin O and radius r *where I is the neutron point of entrance into the system, α the scattering angle,* z *the polar angle defining the point of exit for the scattered neutron and ζ the tilting angle of the secondary detector S2.*

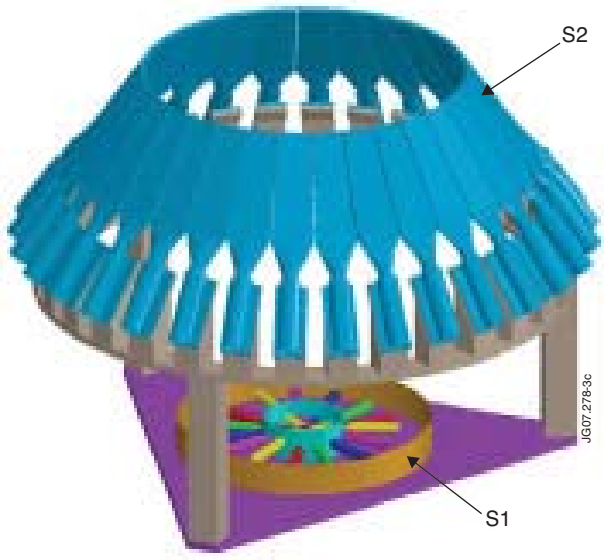

Figure 3: Schematic of the TOFOR spectrometer showing a primary set of 5 S1 scintillators in the collimated neutron beam entering from below, and a secondary set of 32 S2 detectors.

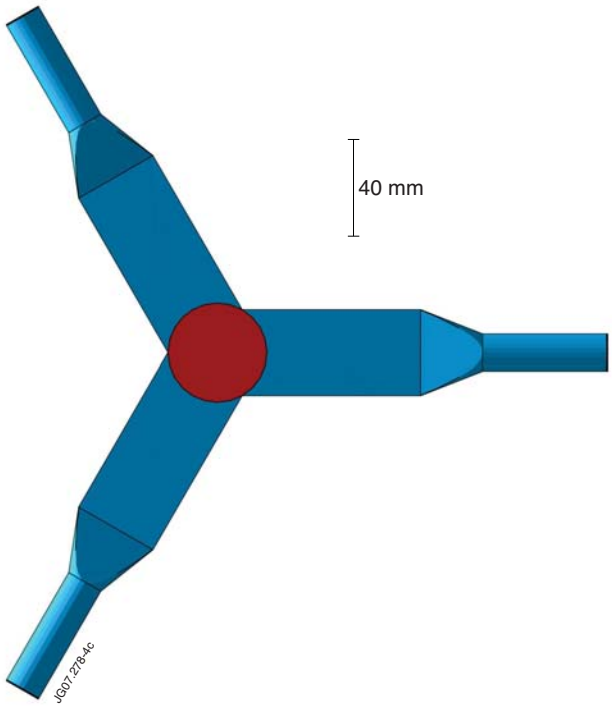

Figure 4: S1 scintillator with light guides attached at 120^{o} angles relative to one another. The scintillator thickness is 5mm,ϕ=40mm and the total length of each light guide 149.3 mm.

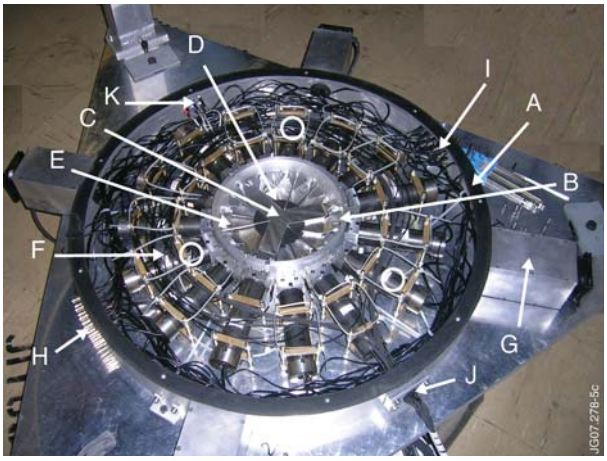

Figure 5: Photograph of the S1 detector assembly mounted on the base plate in the outer (A) and inner (B) enclosures with the lid removed. Identified parts are (C) scintillators with light guides, (D) black cardboard, (E) light fiber guiding pipe, (F) PM holder tube, (G) cooling fan, and feed-throughs for (H) high voltage cables, (I) signal cables, (J) optical fibers and (K) temperature probe cables (at positions indicated by circles).

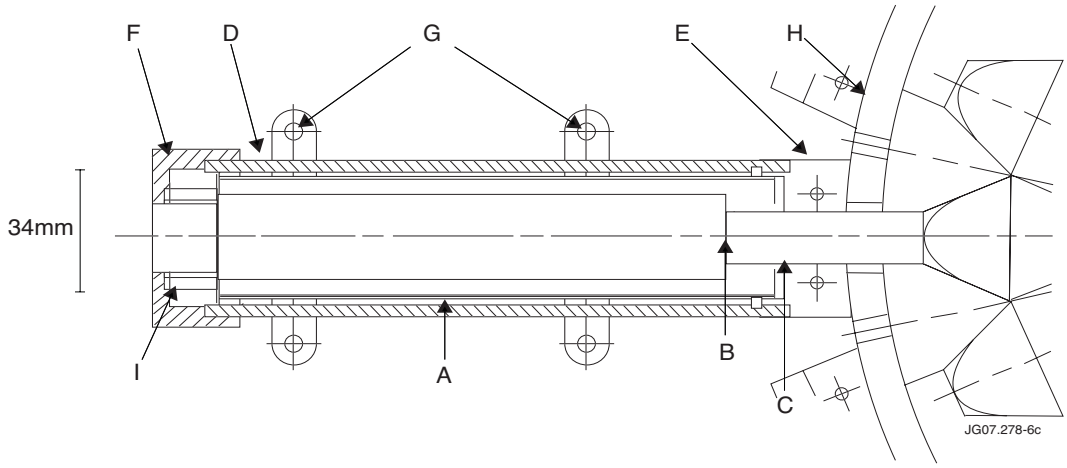

Figure 6: Drawing of the S1 PM tube assembly showing the interface between the PM tube (A), the optical pad (B) and the light guide (C) and the surrounding mounting structure. The parts are (D) a soft iron holder tube with the PM tube on the inside, (E) a separate front piece firmly attached to the light guide, (F) a separate back piece held in place by screws, (G) two holder bar pairs on screws attached to the base plate, (H) the S1 central enclosure ring and (I) a spring pushing the PM tube towards the light guide.

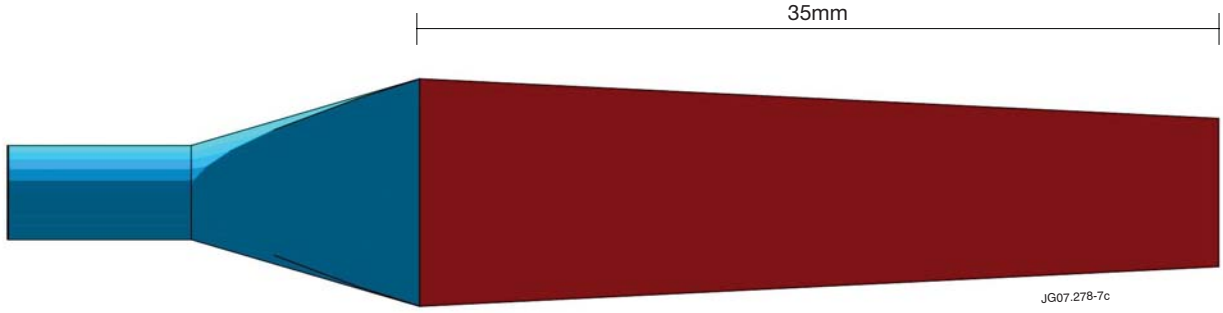

Figure 7: S2 scintillator (right) with attached light guide (left) of fish tail geometry with circular (f=40 mm) cross section facing the PM tube and rectangular (15×134.7mm^2) cross section facing the scintillator (figure not to scale).

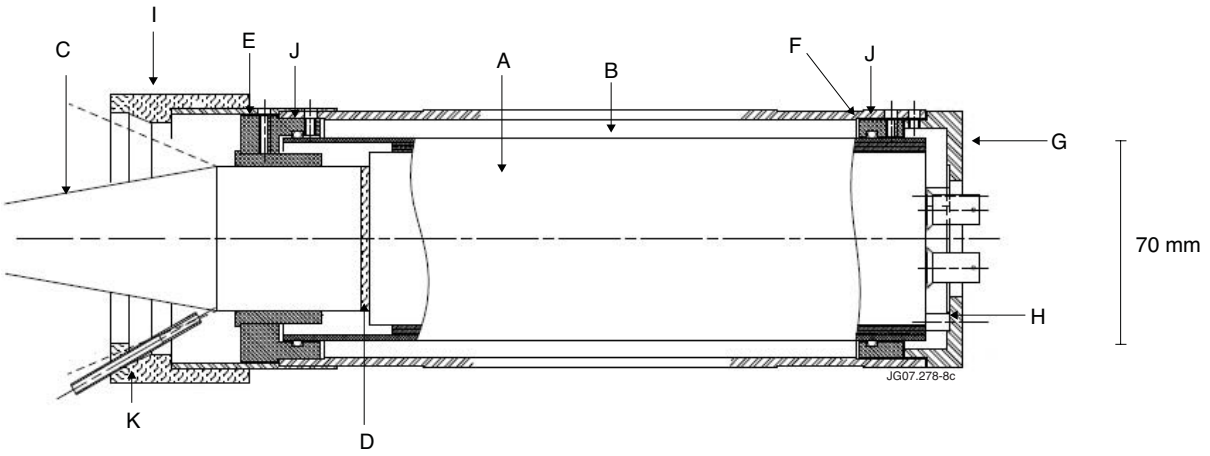

Figure 8: Schematic of an S2 detector showing the PM tube (A) in its soft iron pipe (B) optically connected to the light guide (C) via a silicone pad (D). Also indicated are the front and back holders (E) and (F), the base cap (G), the springs (H), the plastic collar (I), the o-rings (J) keeping the PM tube in place and the light fiber guiding pipe (K).

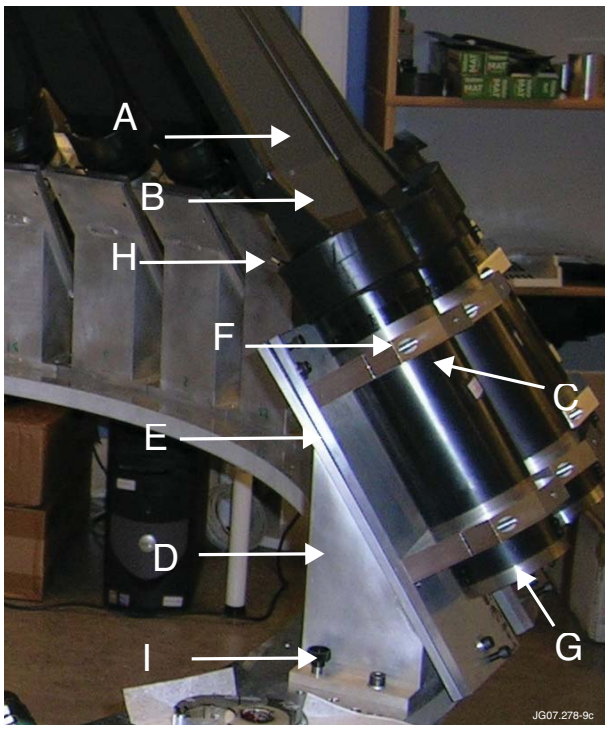

Figure 9: The S2 detector module consisting of (A) scintillator, (B) light guide, (C) PM tube soft iron pipe, (D) support structure, (E) adjustable plate (tilting angle, direction and distance), (F) strap holder (for longitudinal adjustment); also shown are (G) PM tube HV and signal cable connectors, (H) optical fiber access to the light guide and (I) alignment bolt.

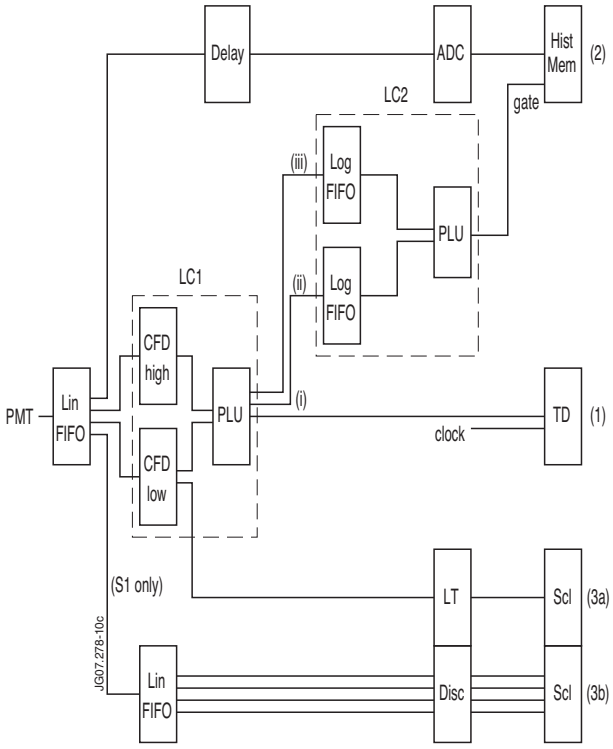

Figure 10: Principles of the TOFOR electronics setup. The three signal lines are (1) the TD line for construction of the flight time spectrum, (2) the ADC line for recording the pulse height spectra from the individual detectors and (3) the scaler line, where signals over set thresholds (one threshold for all scintillators (3a), four extra for each S1 detector (3b)) are counted. The logic circuits LC1 and LC2 as well as the PLU logic outputs (i), (ii), and (iii) are explained in the text.

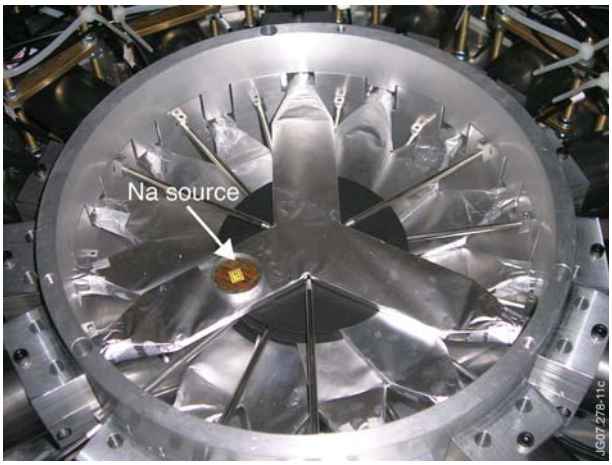

Figure 11: Photograph of the central S1 enclosure with ^{22}Na source ($T_{1/2}$=2.605 years) in place on the top S1 detector layer. Also visible are the aluminum wrapped scintillator/light-guide assemblies with interposed black cardboard sheets besides light fiber guiding tubes.

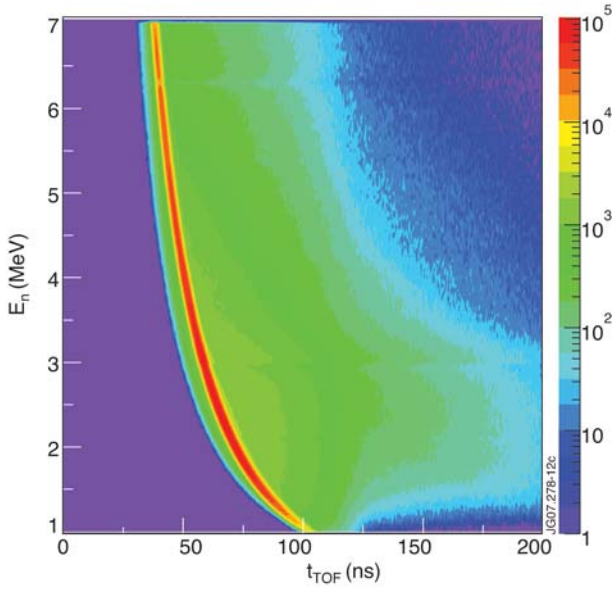

Figure 12: The response matrix R_n for TOFOR showing the t_{TOF} spectrum as a function of simulated neutron energy E_n.

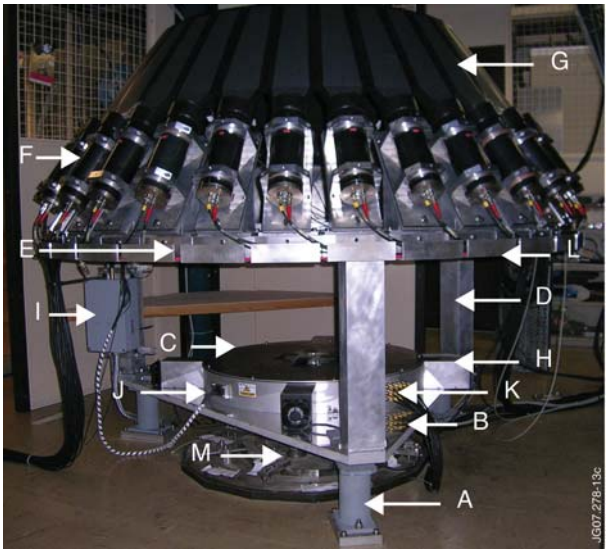

Figure 13: Photograph of TOFOR in the JET roof laboratory with some of the main components identified: The TOFOR legs (A), the base plate (B), the S1 enclosure (C), the legs (D), the support ring (E) and the S2 detector holders (F) with S2 scintillators (G). Also shown are the S1 cooling fans (H), the optical fiber connection box (I), the S1 optical fiber (J) and signal cable (K) feed-throughs and the S2 cable tray (L); (M) is the top of neutron collimator in the roof laboratory floor.

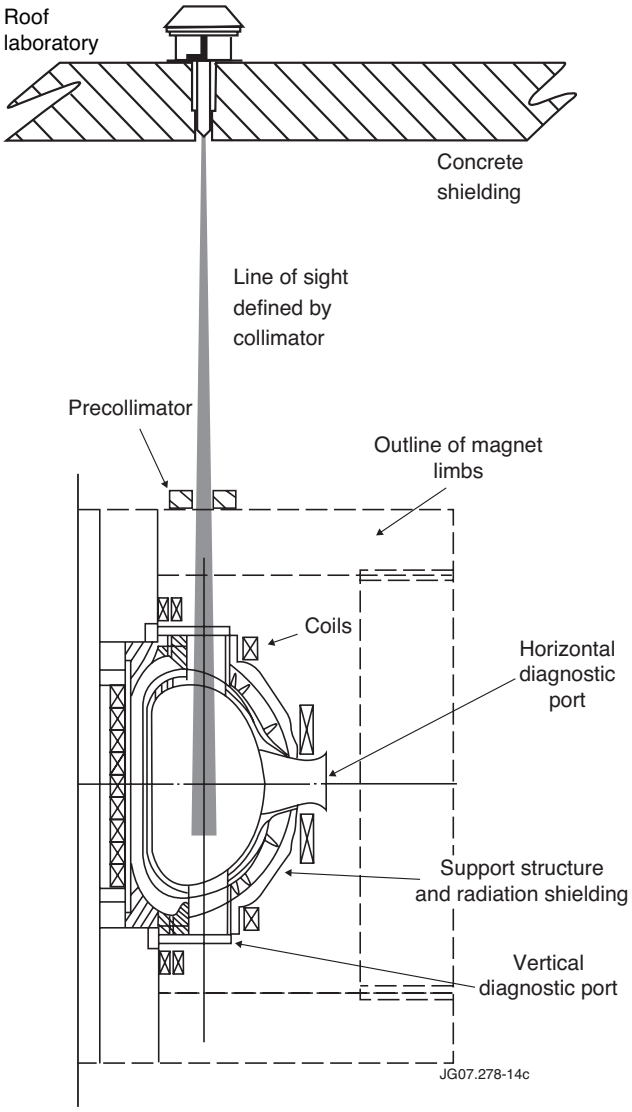

Figure 14: Vertical TOFOR line-of-sight from the roof laboratory into the JET tokamak (poloidal cross section) as defined by the main (1.90-m long) collimator in the concrete shielding. Courtesy of EFDA-JET; Figure: EFDA-JET.

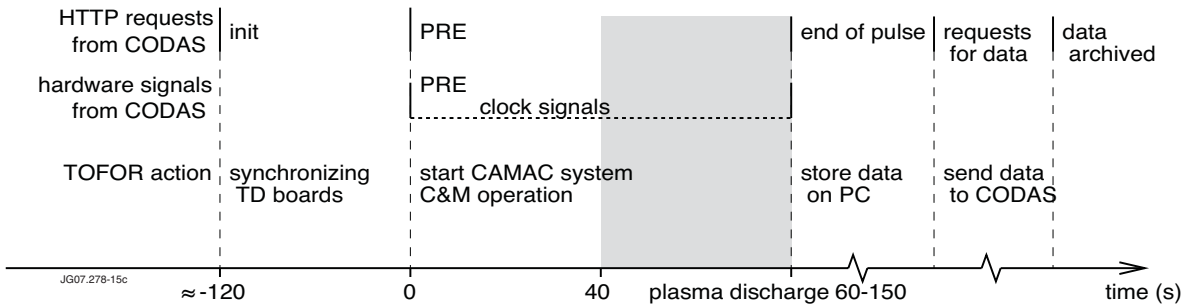

Figure 15: TOFOR-CODAS communication signals as a function of time as part of the data recording process for JET plasma discharges. HTTP requests and trigger (hardware) signals from CODAS and their connection to TOFOR DAQ actions are indicated.

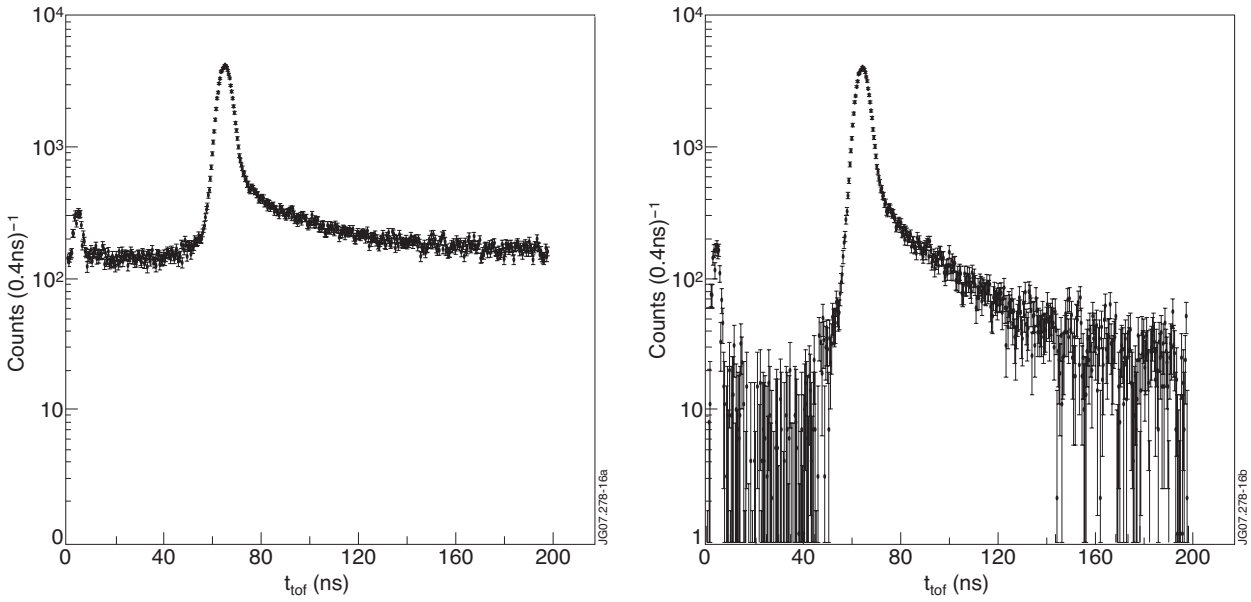

Figure 16: Measured t_{TOF} spectrum using TOFOR to observe the neutron emission from a JET plasma (Pulse No: 69093) of deuterium heated through NB and RF power injection. Shown are the data before (a) and after (b) subtraction of admixed accidental events.

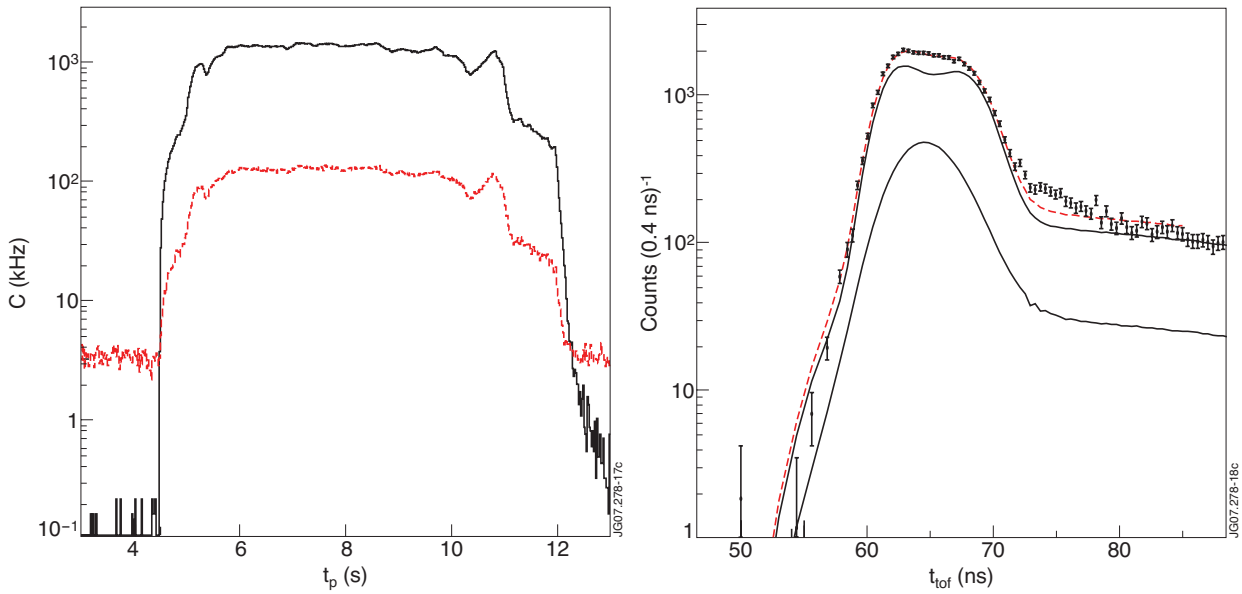

Figure 17: Summed measured single rates as functions of elapsed plasma time t_P for the 5 S1 and 32 S2 detectors of TOFOR for Pulse No:69093 (upper and bottom curves, $C_1(t)$ and $C_2(t)$). The results were obtained with the time digitizer cards using a time binning of 20 ms.

Figure 18: Example of reduced t_{TOF} spectrum obtained with TOFOR for the neutron emission from a JET deuterium plasma (Pulse No:68396) with NB power injection. The lower curve represents the thermal component, the middle the beam component and the top one (that follows the measurement points) represents the summed fit.

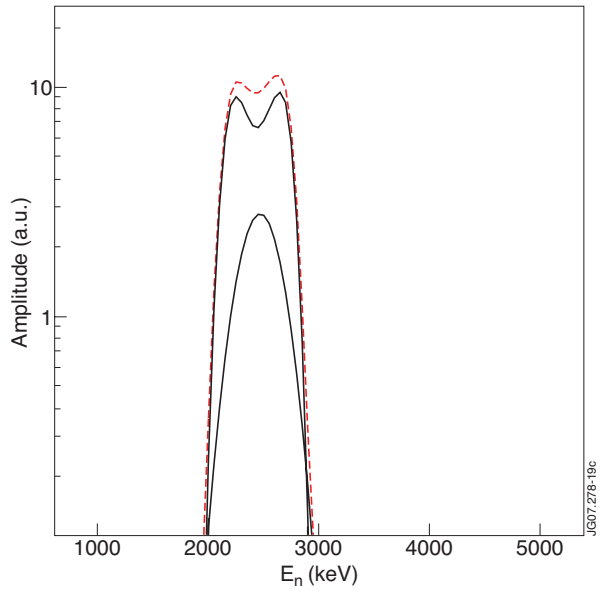

Figure 19: The neutron spectrum extracted from the data in Figure 18 using a least square fitting Again, the lower curve is the thermal component, the middle curve the beam component and the top curve the summed fit.

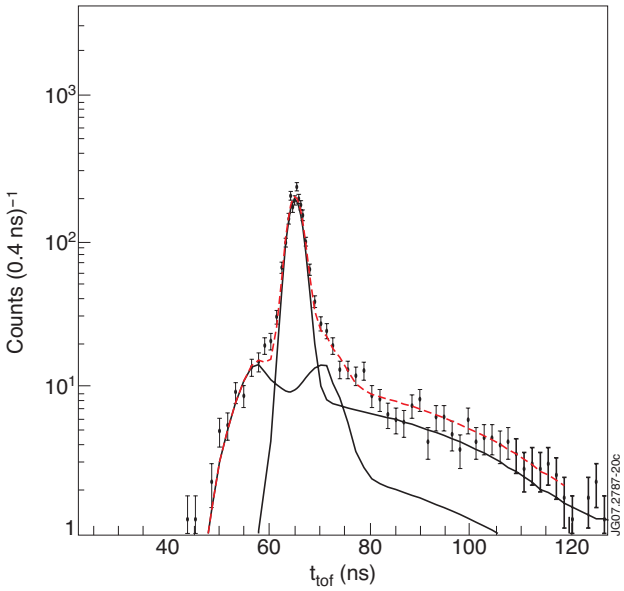

Figure 20: Example of reduced t_{TOF} spectrum obtained with TOFOR for the neutron emission from a JET deuterium plasma (Pulse No: 69529) with RF power injection. The double-peaked curve represents the RF component, the low single-peaked one the thermal component and the top one (that follows the measurement points) the summed fit.

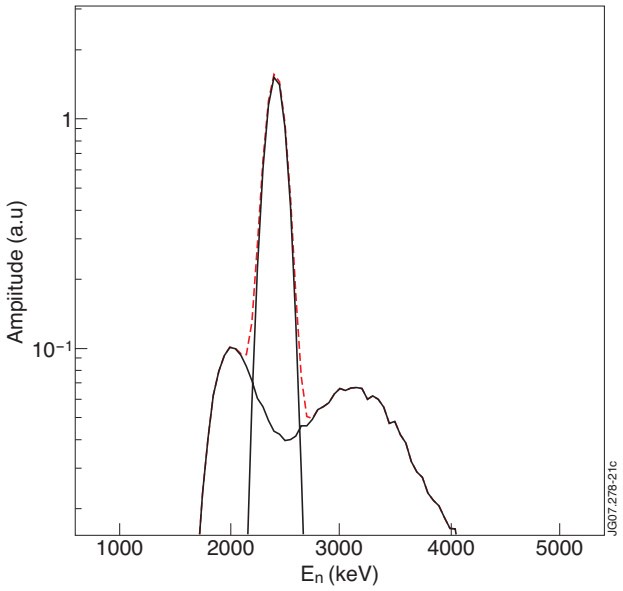

Figure 21: The neutron spectrum extracted from the data in Figure 20 using a least square fitting. Again, the double-peaked curve represents the RF component, the narrow single-peaked one the thermal component and the top curve the fitted sum.